Coupled dipole method determination of the electromagnetic force on a particle over a flat dielectric substrate

P. C. Chaumet and M. Nieto-Vesperinas
Instituto de Ciencia de Materiales de Madrid, Consejo Superior de investigaciones Cientificas, Campus de Cantoblanco, Madrid 28049, Spain
(Received 13 October 1999; revised manuscript received 13 December 1999)

We present a theory to compute the force due to light upon a particle on a dielectric plane by the coupled dipole method. We show that, with this procedure, two equivalent ways of analysis are possible, both based on Maxwell's stress tensor. The interest in using this method is that the nature and size or shape of the object can be arbitrary. Even more, the presence of a substrate can be incorporated. To validate our theory, we present an analytical expression of the force due to the light acting on a particle either in presence, or not, of a surface. The plane wave illuminating the sphere can be either propagating or evanescent. Both two- and three-dimensional calculations are studied.

I. INTRODUCTION

The demonstration of mechanically acting upon small particles with radiation pressure was done by Ashkin.[1,2] A consequence of these works was the invention of the optical tweezer for nondestructive manipulation of suspended particles[3] or molecules and other biological objects.[4–6] Recently, these studies have been extended to the nanometer scale,[7–12] and multiple particle configurations based on optical binding have been studied.[13–17] Also, the effect of evanescent waves created by total internal reflection on a dielectric surface on which particles are deposited was studied in Ref. 18. However, the only theoretical interpretation of such a system is given in Refs. 19 and 20. In Ref. 19 no multiple interaction of the light between the particles and the dielectric surface was taken into account. On the other hand, in Ref. 20 a multiple scattering numerical method was put forward limited to a two-dimensional (2D) configuration.

It is worth remarking here that several previous theoretical works on optical forces usually employ approximations depending on the radius of the particle; if the particle is electrically small it has been usual to split the force into three parts: the gradient, scattering, and absorbing forces.[21] However, a rigorous and exact calculation requires the use of Maxwell's stress tensor. We shall use it in this paper. Some work has been done in free space,[7,22] or for a spherical particle over a dielectric surface illuminated by a Gaussian beam.[23]

We shall present, therefore, a detailed theoretical analysis in three dimensions of how the optical force is built on the multiple interaction of light with the particle and the dielectric surface. This will be done whatever its size, shape, or permittivity. To this end, we shall make use of the coupled dipole method (CDM), whose validity was studied in detail in Ref. 25.

In Sec. II we present the CDM, and two possibilities that arise with this method to compute the force by means of Maxwell's stress tensor. Concerning the first possibility, in Sec. II A we use Maxwell's stress tensor directly and perform the surface integrations. As regards the second possibility, we present in Sec. II B the dipole approximation on each subunit of discretization for the numerical calculations. Since, however, these methods are somewhat cumbersome from a numerical point of view, we have introduced in Sec. III an analytical calculation for the force due to the light on a electrically small particle in the presence of the surface. Results are illustrated in three dimensions in Sec. III A (a little sphere) and in two dimensions in Sec. III B (a small cylinder). In Sec. IV we compute the force with the CDM and validate these calculations on electrically small particles by means of the analytical solution presented in Sec. III. After this validation of the CDM on little particles, we present in Sec. IV C calculations on larger particles.

II. ELECTROMAGNETIC FORCE COMPUTED WITH THE COUPLED DIPOLE METHOD

The CDM was introduced by Purcell and Pennypacker in 1973 for studying the scattering of light by nonspherical dielectric grains in free space.[26] This system is represented by a cubic array of N polarizable subunits. The electric field $\mathbf{E}(\mathbf{r}_i,\omega)$ at each subunit position $\mathbf{r}_i$ can be expressed as

$$\mathbf{E}(\mathbf{r}_i,\omega)=\mathbf{E}_0(\mathbf{r}_i,\omega)+\sum_{j=1}^{N}[\mathbf{S}(\mathbf{r}_i,\mathbf{r}_j,\omega)+\mathbf{T}(\mathbf{r}_i,\mathbf{r}_j,\omega)]\alpha_j(\omega)\mathbf{E}(\mathbf{r}_j,\omega), \quad (1)$$

where $\mathbf{E}_0(\mathbf{r}_i,\omega)$ is the field at the position $\mathbf{r}_i$ in the absence of the scattering object, $\mathbf{T}$ is the linear response to a dipole in free space,[27] and $\mathbf{S}$ represents the linear response of a dipole in the presence of a surface in front of which the particle is placed (see Fig. 1). We take the weak form of the CDM, as in our configuration the strong form does not adapt.[28] However, in fact for very small discretization subunits, the difference of results derived from the strong and weak forms is not significant. The derivation of $\mathbf{S}$ is extensively developed in Refs. 29 and 30. $\alpha_j(\omega)$, the polarizability of the subunit j, is expressed as:

$$\alpha_j(\omega)=\alpha_j^0(\omega)/[1-(2/3)ik_0^3\alpha_j^0(\omega)], \quad (2)$$

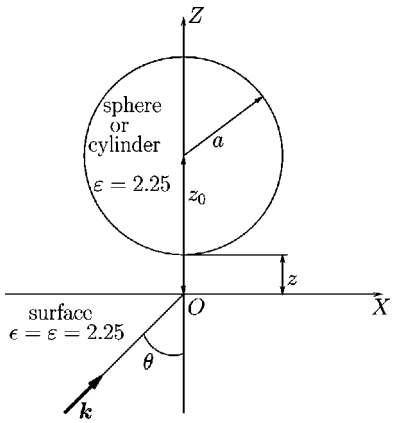

FIG. 1. Geometry of the configuration considered in this paper: sphere, or cylinder, of radius a on a dielectric flat surface. The relative permittivity is $\varepsilon = 2.25$ both for the sphere (or the cylinder) and the surface. The wavelength used is $\lambda = 632.8$ nm in vacuum and the incident wave vector $\mathbf{k}$ is in the XZ plane.

where $k_0 = |\mathbf{k}_0| = \omega/c$ ($\mathbf{k}_0$ being the incident wave vector of the electromagnetic field in vacuum) and $\alpha_j^0(\omega)$ is given by the Clausius-Mossotti relation:

$$\alpha_j^0(\omega) = \frac{3d^3}{4\pi}\frac{\varepsilon(\omega)-1}{\varepsilon(\omega)+2}. \tag{3}$$

In Eq. (3) d is the spacing of lattice discretization and $\varepsilon(\omega)$ stands for the relative permittivity of the object. Let us remark that the polarizability is expressed according to Eq. (2) as defined by Draine.[31] The term $(2/3)ik_0^3\alpha_j^0(\omega)$ is the radiative reaction term, necessary for the optical theorem to be satisfied and for a correct calculation of forces via the CDM.[32]

Once the values of $\mathbf{E}(\mathbf{r}_i,\omega)$ are obtained by solving the linear system, Eq. (1) (whose size is $3N\times 3N$), it is easy to compute the field at an arbitrary position $\mathbf{r}$:

$$\mathbf{E}(\mathbf{r},\omega) = \mathbf{E}_0(\mathbf{r},\omega) + \sum_{j=1}^{N} [\mathbf{S}(\mathbf{r},\mathbf{r}_j,\omega) + \mathbf{T}(\mathbf{r},\mathbf{r}_j,\omega)]\alpha_j(\omega)\mathbf{E}(\mathbf{r}_j,\omega). \tag{4}$$

The computation of the force also requires the magnetic field radiated by the scattering object. We obtain it through Faraday's equation, $\mathbf{H}(\mathbf{r},\omega) = c/(i\omega)\boldsymbol{\nabla}\times\mathbf{E}(\mathbf{r},\omega)$.

A. Force computed with Maxwell's stress tensor

The force $\mathbf{F}$ on an object due to the electromagnetic field[33] is computed from Maxwell's stress tensor:[34]

$$\mathbf{F} = 1/(8\pi)\mathrm{Re}\left[\int_S \{[\mathbf{E}(\mathbf{r},\omega)\cdot\mathbf{n}]\mathbf{E}^*(\mathbf{r},\omega) + [\mathbf{H}(\mathbf{r},\omega)\cdot\mathbf{n}]\mathbf{H}^*(\mathbf{r},\omega) - 1/2[|\mathbf{E}(\mathbf{r},\omega)|^2 + |\mathbf{H}(\mathbf{r},\omega)|^2]\mathbf{n}\}d\mathbf{r}\right], \tag{5}$$

where S is a surface enclosing the object, $\mathbf{n}$ is the local outward unit normal, the asterisk denotes the complex conjugate, and Re represents the real part of a complex number. Let us notice that Eq. (5) is written in CGS units for an object in vacuum, and so will be given all forces presented in Sec. IV. To apply Eq. (5) with the CDM, we must first solve Eq. (1) to obtain $\mathbf{E}(\mathbf{r}_i,\omega)$ at each dipole position, and then, through Eq. (4) and the Faraday equation, the electromagnetic field is computed at any position $\mathbf{r}$ of S. This enables us to numerically perform the two-dimensional quadrature involved in Eq. (5).

B. Force determined via the dipolar approximation

Let us consider a small spherical particle with a radius smaller than the wavelength. Then the u component of the force can be written in the dipole approximation:[35,32]

$$F_u(\mathbf{r}_0) = (1/2)\mathrm{Re}\sum_{v=1}^{3}\left\langle p_v(\mathbf{r}_0,\omega)\frac{\partial E_v^*(\mathbf{r}_0,\omega)}{\partial u}\right\rangle, \quad u = 1,2,3 \tag{6}$$

where $\mathbf{r}_0$ is the position of the center of the sphere and u and v stand for the components along x, y, or z. We discretize the object into N small dipoles $\mathbf{p}(\mathbf{r}_i,\omega)$ ($i = 1,\ldots,N$) so that it is possible to compute the force on each dipole from Eq. (6). Hence, to obtain the total force on the particle it suffices to sum the contributions $\mathbf{F}(\mathbf{r}_i)$ from all of the dipoles. To use this method it is necessary to know $\partial E_v(\mathbf{r}_i,\omega)/\partial u$ at each discretization subunit. On performing the derivative of Eq. (1) we obtain

$$\left(\frac{\partial\mathbf{E}(\mathbf{r},\omega)}{\partial\mathbf{r}}\right)_{\mathbf{r}=\mathbf{r}_i} = \left(\frac{\partial\mathbf{E}_0(\mathbf{r},\omega)}{\partial\mathbf{r}}\right)_{\mathbf{r}=\mathbf{r}_i} + \sum_{j=1}^{N}\left\langle\frac{\partial}{\partial\mathbf{r}}[\mathbf{S}(\mathbf{r},\mathbf{r}_j,\omega) + \mathbf{T}(\mathbf{r},\mathbf{r}_j,\omega)]\right\rangle_{\mathbf{r}=\mathbf{r}_i}\alpha_j(\omega)\mathbf{E}(\mathbf{r}_j,\omega). \tag{7}$$

Thus, the derivative of the field at $\mathbf{r}_i$ requires that of $\mathbf{E}_0(\mathbf{r}_i,\omega)$ and that of $\mathbf{T}$ and $\mathbf{S}$ for all pairs $(\mathbf{r}_i,\mathbf{r}_j)$. Hence we now have two tensors with 27 components each. It is important to notice that the derivative of the field at $\mathbf{r}_i$ has been directly computed from just the field at this position $\mathbf{r}_i$, so it is not computed in a self-consistent manner. To have the required self-consistence for the derivative, it is necessary to perform in Eq. (1) a multipole expansion up to second order. Then, this equation must be written up to the quadrupole order after taking its derivative. As a result, we obtain a linear system whose unknowns are both the electric field and its derivative. The disadvantage of this method is that the size of the linear system increases up to $12N\times 12N$ and requires the computation of the second derivative of $\mathbf{T}$ and $\mathbf{S}$ (81 components). More information about the CDM by using the multipole expansion can be found in Ref. 25.

In what follows, we shall denote CDM-A the force computed directly from Maxwell's stress tensor Eq. (5) and CDM-B the force obtained on using the field derivative Eq. (6). The advantages of these two methods is that they are not restricted to a particular shape of the object to be discretized. Furthermore, this object can be inhomogeneous, metallic, or in a complex system whenever it is possible to compute its linear response to a dipole.

III. FORCE ON A DIPOLAR PARTICLE

A. The three-dimensional case: A sphere

Equation (1) with $N=1$, taking the surface into account, gives for the field at the position $\mathbf{r}_0=(x_0,y_0,z_0)$ of the sphere of a radius a:

$$\mathbf{E}(\mathbf{r}_0,\omega)=[\mathbf{I}-\alpha(\omega)\mathbf{S}(\mathbf{r}_0,\mathbf{r}_0,\omega)]^{-1}\mathbf{E}_0(\mathbf{r}_0,\omega), \tag{8}$$

where $\mathbf{I}$ is the unit tensor and $\alpha(\omega)$ the polarizability of the sphere according to Eq. (2) with $\alpha_0(\omega)=a^3[\varepsilon(\omega)-1]/[\varepsilon(\omega)+2]$. We notice that $\mathbf{S}$ is purely diagonal and depends only on the distance z_0 between the center of the sphere and the surface (see Fig. 1). We also assume that the sphere is near the surface, and hence $\mathbf{S}$ can be used in the static approximation ($k_0=0$, we shall discuss the validity of this approximation in Sec. IV). Therefore, the components of this tensor become $S_{xx}=S_{yy}=-\Delta/(8z_0^3)$ and $S_{zz}=-\Delta/(4z_0^3)$, with $\Delta=(1-\epsilon)/(1+\epsilon)$ representing the Fresnel coefficient of the surface. Since we consider the object in the presence of a surface with a real relative permittivity, Δ is real. As shown by Fig. 1, the light incident wave vector $\mathbf{k}_0$ lies in the XZ plane. Therefore, there is no force in the Y direction. On using Eqs. (6) and (8), and assuming the incident field $\mathbf{E}_0$ above the surface to be a plane wave either propagating or evanescent, depending on the illumination angle θ, the components of the force on the sphere can be written as

$$F_x=\frac{\mathrm{Re}}{2}\left[4\alpha z_0^3(ik_x)^*\left(\frac{2|E_{0x}|^2}{8z_0^3+\alpha\Delta}+\frac{|E_{0z}|^2}{4z_0^3+\alpha\Delta}\right)\right], \tag{9}$$

$$F_z=|E_{0x}|^2\frac{\mathrm{Re}}{2}\left(\frac{8z_0^3\alpha(ik_z)^*}{8z_0^3+\alpha\Delta}+\frac{12z_0^2|\alpha|^2\Delta}{|8z_0^3+\alpha\Delta|^2}\right)+|E_{0z}|^2\frac{\mathrm{Re}}{2}\left(\frac{4z_0^3\alpha(ik_z)^*}{4z_0^3+\alpha\Delta}+\frac{6z_0^2|\alpha|^2\Delta}{|4z_0^3+\alpha\Delta|^2}\right) \tag{10}$$

for p polarization and

$$F_x=|E_{0y}|^2\frac{\mathrm{Re}}{2}\left[\frac{8z_0^3\alpha(ik_x)^*}{8z_0^3+\alpha\Delta}\right], \tag{11}$$

$$F_z=|E_{0y}|^2\frac{\mathrm{Re}}{2}\left(\frac{8z_0^3\alpha(ik_z)^*}{8z_0^3+\alpha\Delta}+\frac{12z_0^2|\alpha|^2\Delta}{|8z_0^3+\alpha\Delta|^2}\right) \tag{12}$$

for s polarization. We see that the advantage of working with the static approximation is that an analytic form of the force is obtained. To see the effect of the incident field only (i.e., without interaction with the surface), we can put $z_0\to\infty$ or $\Delta=0$ in Eqs. (9)–(12). The forces are then expressed as

$$F_x=|E_0|^2\frac{\mathrm{Re}}{2}[\alpha(ik_x)^*], \tag{13}$$

$$F_z=|E_0|^2\frac{\mathrm{Re}}{2}[\alpha(ik_z)^*], \tag{14}$$

with $|E_0|^2=|E_{0y}|^2$ for s polarization and $|E_0|^2=|E_{0x}|^2+|E_{0z}|^2$ for p polarization. Equations (13) and (14) show a spherical symmetry, and hence the results both in p and s polarization are the same.

If we look at Fig. 1, we see that the incident field above the surface always has k_x real, but k_z can be either real (propagating wave) or imaginary (evanescent wave when $\theta>\theta_c$, where θ_c is the critical angle defined as $\sqrt{\epsilon}\sin\theta_c=1$). Hence, all forces in the X direction have the form $A\,\mathrm{Re}[\alpha(ik_x)^*]$, where A is always a positive number. In using Eq. (2) we find that $\mathrm{Re}[\alpha(ik_x)^*]\simeq(2/3)\alpha_0^2k_0^3k_x$ [we have assumed that $(4/9)k_0^6\alpha_0^2\ll1$; in fact, this expression is about 6.6×10^{-7} for $a=10$ nm, $\lambda=632.8$ nm, and $\varepsilon=2.25$; thus this approximation is perfectly valid]. Hence, whatever the field, either propagating or evanescent, and whether the system is in the presence of a surface or in free space, the force in the X direction is always along the incident field.

From Eq. (14) and from the discussion above, it is easy to see that in the absence of interfaces the force is positive for a propagating incident wave (k_z real). In the case of an evanescent incident wave, $k_z=i\gamma$ with $\gamma>0$, and hence the force becomes $F_z=-\gamma\alpha_0|E_0|^2/2$; namely, the sphere is attracted towards the higher intensity field. Concerning the force along the Z direction, its sign will depend on the nature of the field and the interaction of the sphere with the surface. We shall discuss this in Sec. IV A.

B. The two-dimensional case: A cylinder

For a cylinder with its axis at (x_0,z_0), parallel to the Y axis (Fig. 1), the electric field at its center is obtained by an equation similar to Eq. (8), but with a different polarizability. With the help of Refs. 36 and 37 we write this polarizability:

$$\alpha_1(\omega)=\frac{\alpha_1^0(\omega)}{1-ik_0^2\pi\alpha_1^0(\omega)/2}\quad\text{with}\quad\alpha_1^0(\omega)=\frac{\varepsilon(\omega)-1}{\varepsilon(\omega)+1}\frac{a^2}{2}, \tag{15}$$

$$\alpha_2(\omega)=\frac{\alpha_2^0(\omega)}{1-ik_0^2\pi\alpha_2^0(\omega)}\quad\text{with}\quad\alpha_2^0(\omega)=[\varepsilon(\omega)-1]\frac{a^2}{4}. \tag{16}$$

The subscripts $i=1$ and 2 correspond to the field perpendicular and parallel to the axis of the cylinder, respectively. The linear response in the presence of a surface in the two dimensional case is given in Ref. 38 for s-polarization and in Ref. 39 for p polarization. Since we address a cylinder with a small radius a and near the surface, we use the static approximation, and then $S_{xx}=S_{zz}=-\Delta/(2z_0^2)$ and $S_{yy}=0$. In the same way as seen before, the force is written as

$$F_x=|E_0|^2\frac{\mathrm{Re}}{2}[\alpha_2(ik_x)^*], \tag{17}$$

$$F_z=|E_0|^2\frac{\mathrm{Re}}{2}[\alpha_2(ik_z)^*] \tag{18}$$

for s polarization and

TABLE I. Force on a sphere of radius $a=10$ nm in free space. Numerical results for different number of subunits N in the CDM-A, CDM-B. Comparison of calculation with the dipolar approximation and Mie's calculation. % (Mie) is the relative difference (in percent) between the exact Mie calculation and the method used.

CDM-A			CDM-B			Dipole approx.		Mie
Force	N	% (Mie)	Force	N	% (Mie)	Force	% (Mie)	Force
2.8119×10^{-22}	81	0.46	2.8338×10^{-22}	81	1.24	2.8027×10^{-22}	0.13	2.7991×10^{-22}
2.8181×10^{-22}	912	0.68	2.8243×10^{-22}	912	0.91			
2.8151×10^{-22}	1791	0.57	2.8194×10^{-22}	1791	0.73			
2.8151×10^{-22}	2553	0.57	2.8186×10^{-22}	2553	0.70			

$$F_x=|E_0|^2\frac{\mathrm{Re}}{2}\left(\frac{2z_0^2\alpha_1(ik_x)^*}{2z_0^2+\alpha_1\Delta}\right), \tag{19}$$

$$F_z=|E_0|^2\frac{\mathrm{Re}}{2}\left(\frac{2z_0^2\alpha_1(ik_z)^*}{2z_0^2+\alpha_1\Delta}+\frac{2z_0|\alpha_1|^2\Delta}{|2z_0^2+\alpha_1\Delta|^2}\right) \tag{20}$$

for p polarization. $|E_0|^2=|E_{0y}|^2$ for s polarization and $|E_0|^2=|E_{0x}|^2+|E_{0z}|^2$ for p polarization. If, again, $z_0\to\infty$ or $\Delta=0$ and there is no interaction between the cylinder and the surface, then we find the same equations as those established for the sphere with only a replacement of α by α_1 or α_2, depending on the polarization. Concerning the force along the X direction, we have the same effect as for the sphere, namely, F_x has the sign of k_x.

IV. NUMERICAL RESULTS AND DISCUSSION

In this section we present numerical results on forces acting on either an electrically small sphere or a small cylinder. Theses forces are normalized in the form $F_u/|E_0|^2$, where F_u is the u component of the force and $|E_0|$ stands for the modulus of the incident field at the center of either the sphere or the cylinder. All calculations are done for a body in glass ($\varepsilon=2.25$), at a wavelength of 632.8 nm, in front of a flat surface ($\epsilon=\varepsilon=2.25$) illuminated from the glass side by internal reflection (Fig. 1).

A. Results for an electrically small sphere

We have first checked our CDM calculation by comparing it with the well known Mie scattering results for a sphere in free space illuminated by a plane wave.[40] The force is

$$\mathbf{F}_{Mie}=\frac{1}{8\pi}|E_0|^2(C_{ext}-\overline{\cos\theta}C_{sca})\frac{\mathbf{k}_0}{k_0}, \tag{21}$$

where C_{ext} denotes the extinction cross section, C_{sca} the scattering cross section, and $\overline{\cos\theta}$ the average of the cosine of the scattering angle. Calculations are done for a sphere of radius $a=10$ nm.

Table I compares the force obtained from the CDM on using, without any approximation, either the method developed in Sec. II A (CDM-A) or that from Sec. II B (CDM-B), and from the dipolar approximation presented in Sec. III A, with the Mie calculation [% (Mie) is the relative difference in percent between the Mie result and the other corresponding method]. For an incident field with $|E_0|=94825$ V/m, which corresponds to a power of 1.19 mW distributed on a surface of 10 μm^2, the force on the sphere in MKSA units is 2.7991×10^{-22} N. One can see that for both CDM-A and CDM-B the convergence is reached even for a coarse discretization, and hence either one of the two CDM approaches can be used. As regards the dipolar approximation, we conclude that it is perfectly valid to use it for a sphere of radius a=10 nm ($a/\lambda<0.016$). Notice that in this article we prefer the Clausius-Mossotti relation with the radiative reaction term to the polarizability defined by Dungey and Bohren[24] as the force obtained in free space for an electrically small sphere is less accurate than the one obtained from the Clausius-Mossotti relation.

Now that we have validated our methods (both analytic and CDM) we proceed to take the surface into account. It should be remarked that with the CDM-A it is not possible to compute the force when the sphere is on the surface. This is because for an observation point very close to the sphere, the electromagnetic field values are affected by the discretization of the sphere, and so the field is not correctly computed. An empirical criterion that we have found[25] is that the electric field must be computed at least at a distance d from the sphere, but this criterion depends on the relative permittivity. For more precision about the dependence of the criterion and the relative permittivity one can look to Ref. 31. With the CDM-B this problem does not occur because with this approach it is not necessary to obtain the field outside the sphere.

In all figures shown next, we plot the force versus the distance z between the sphere (or the cylinder, see Sec. IV B)

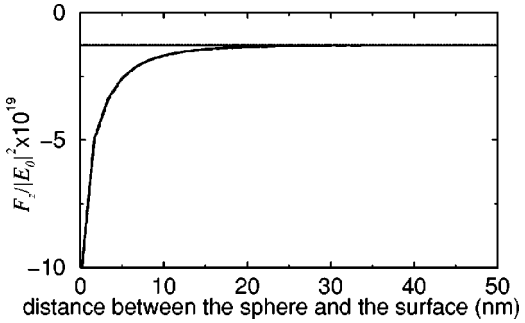

FIG. 2. Normalized force in the Z direction on the sphere of $a=10$ nm versus distance Z. The angle of incidence of illumination is $\theta=42°$ in p polarization. The full line represents the exact calculation with CDM-B, the dashed line corresponds to the static approximation with CDM-B, and the dotted line is the calculation without interaction between the sphere and the surface.

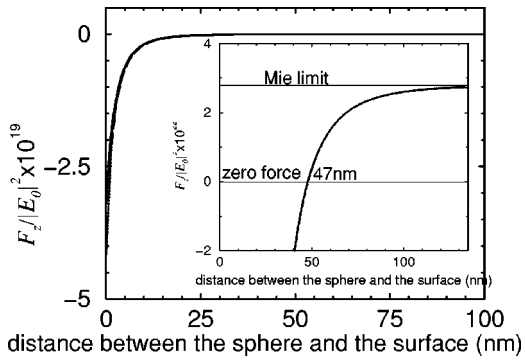

FIG. 3. Normalized force in the Z direction on a sphere of radius $a=10$ nm. The full line corresponds to the dipole approximation, the dashed line to the CDM-A, and the dotted line to the CDM-B. The angle of incidence is $\theta=0°$. The inset shows the force near $z=50$ nm. We show the zero force and the force computed from Mie's limit with Eq. (21).

and the plane (notice that we represent by z_0 the distance between the center of the sphere, or cylinder, and the plane). The calculation using the dipole approximation, as well as the CDM (A or B), has been done with the static approximation for the linear response of a dipole in the presence of a surface (SALRS). However, the distance between the sphere and the surface goes generally up to 100 nm. In order to justify the study of the force at distances about 100 nm between the sphere and the plane through a calculation done in the static approximation, we plot in Fig. 2 the normalized force F_z for p polarization, with a sphere of radius $a=10$ nm, at an angle of incidence $\theta=42°$, without any approximation with the CDM-A (namely, taking into account all retardation effects) with the SALRS, and with the approximation in which no interaction between the sphere and the surface is considered. The difference between SALRS and the exact calculation is less than 1.5%. This is in fact logical. Near the surface, the SALRS is correct, far from the surface. However, **S** in the exact calculation is significantly different from **S** derived from a static approximation. Nevertheless, for distances larger than $z=30$ nm the curves overlap because the sphere does not ''feel'' the substrate at this distance. This is manifested by a difference of only 2% between the exact calculation result and that computed without addressing the surface (horizontal line).

Figure 3 shows the normalized force for light at an angle of incidence $\theta=0°$. The curves corresponding to CDM-A and CDM-B are similar, and the dipole approximation appears slightly above when the sphere is close to the surface. This may seem strange at first sight in view of the good results presented in Table I (we will discuss it later). We can see that although the illuminating wave is propagating, if the sphere is near the surface, it is attracted towards it, opposite to the propagation direction. To understand this, we look at Eq. (12), established with the dipole approximation with the values $k_x=0$, $k_z=k_0$, and $E_{0z}=0$, which corresponds to $\theta=0°$. After some approximations [namely $(4/9)k_0^6\alpha_0^2 \ll 1$, which implies $|\alpha|^2 \simeq \alpha_0^2$], the force can be written:

$$F_z=\frac{|E_0|^2 64 z_0^6}{|8z_0^3+\alpha\Delta|^2}\left(\alpha_0^2 k_0^4/3+\frac{3\alpha_0^2\Delta}{32 z_0^4}\right). \tag{22}$$

The factor before the parentheses of Eq. (22) corresponds to the intensity of the field at the position of the sphere. The first term in the parentheses of this equation is due to the light scattering on the particle (as in free space) and is always positive. The second term in the parentheses is always negative as $\Delta<0$. Therefore, the relative weight of the two terms in Eq. (22) determines the direction of F_z. F_z given by Eq. (22), becomes zero for

$$z_0^4=\frac{9(\varepsilon-1)}{32k_0^4(\varepsilon+1)}. \tag{23}$$

Hence, in our example we find $z_0=57$ nm. Below the value of Eq. (23) the force is attractive towards the surface, and above this value the sphere is pushed away. This is seen in the inset of Fig. 3 which enlarges those details. We find $F_z=0$ at $z=47$ nm namely at $z_0=(47+10)$ nm$=57$ nm, which is exactly the same value previously found. Physically, the attraction of the sphere is due to the second term of Eq. (22), which corresponds to the interaction of the dipole with its own evanescent field reflected by the surface. Now we can explain the discrepancy between the dipole approximation and the CDM as regards the good results obtained in free space. In fact, when the computation is done in free space the field can be considered uniform over a range of 20 nm. However, in an evanescent field, the applied field is not uniform inside the sphere and the Clausius-Mossotti relation is less adequate. Hence the dipole approximation departs more from the exact calculation. However, when the sphere is out from the near field zone, the three methods match well (see the inset of Fig. 3). We can also see in the

TABLE II. Force on a finite cylinder of radius $a=10$ nm in free space. The discretization interval is $d=4$ nm. Numerical results are presented for different lengths L of the cylinder for both CDM-A and CDM-B. Comparison is made with both the dipolar approximation and Mie's calculation. % (Mie) is the relative difference between the exact Mie calculation for an infinite cylinder and the method used. Calculations are done for the field perpendicular to the axis of the cylinder.

CDM-A			CDM-B			Dipole approx.		Mie
Force	L (nm)	% (Mie)	Force	L (nm)	% (Mie)	Force	% (Mie)	Force
2.1540×10^{-13}	197	24	2.1625×10^{-13}	197	24	2.8433×10^{-13}	0.27	2.8354×10^{-13}
2.9906×10^{-13}	391	5.47	3.0013×10^{-13}	391	5.85			
2.7907×10^{-13}	777	1.58	2.8000×10^{-13}	777	1.25			
2.8661×10^{-13}	1164	1.08	2.8756×10^{-13}	1164	1.42			
2.8347×10^{-13}	1551	0.03	2.8439×10^{-13}	1551	0.30			

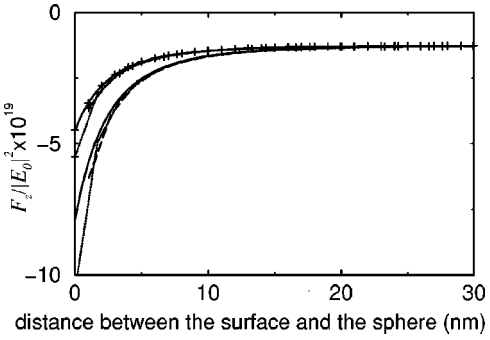

FIG. 4. Normalized force in the Z direction acting on the sphere with $a=10$ nm. The angle of incidence $\theta=42°$ is larger than the critical angle $\theta_c=41.8°$. The full line corresponds to the dipole approximation, the dashed line to the CDM-A, and the dotted line to the CDM-B. Curves without symbols are for p polarization, and those with symbol + are for s polarization.

inset of Fig. 3 that these three curves tend towards the Mie limit because at large distance there is no interaction with the surface.

Figure 4 shows the z component of the normalized force when the incident wave illuminated at $\theta=42°>41.8°=\theta_c$. Then, for s polarization we can write Eq. (12) as

$$F_z=\frac{|E_{0y}|^2}{|8z_0^3+\alpha\Delta|^2}[-4z_0^3\gamma\alpha_0(\alpha_0\Delta+8z_0^3)+6z_0^2\alpha_0^2\Delta]. \tag{24}$$

It is easy to see that for a dielectric sphere both the first and second terms within the brackets of Eq. (24) are always negative. Hence, the sphere is always attracted towards the surface (the same reasoning can be done for p polarization). Near the surface the force becomes larger because of the interaction of the sphere with its own evanescent field. We notice that the normalized force becomes constant at larger z. This constant reflects the fact that the force decreases as $e^{-2\gamma z}$ from the surface.

B. Results for a small cylinder

Let us now address an infinite cylinder. Since the CDM method used here works in three dimensions, we have computed the force on a finite length cylinder. In order to verify this approximation, we once again compare the force, obtained in free space from the CDM with different cylinders lengths, with that from a calculation done with the dipole approximation established in Sec. III B, and that from an exact calculation for an infinite cylinder[40] (i.e., the well known 2D version for cylinders of the Mie calculation for spheres). We consider a radius of the cylinder, $a=10$ nm, with the same spacing lattice as for the case of the sphere, namely 81 subunits. We have seen that this value of $d=4$ nm gives consistent results. In all cases we compute the force per unit length of the cylinder.

The first case addressed is with the electric field perpendicular to the axis of the cylinder (p polarization). The results are given in the Table II. The second case considered is with the electric field parallel to the axis of the cylinder (s polarization) in Table III.

We notice that the dipole approximation gives the correct results for p polarization, but it is worse for s polarization. If we compare CDM-A and CDM-B, we see that they both give the same results. But we also see that the length of the cylinder has a great influence, although up to a different extent according to whether we deal with p or s polarization. For p polarization, the simulation of an infinite cylinder becomes correct at $L\simeq\lambda/2$ and for s polarization only it is so at $L\simeq 2\lambda$. This can be understood by the fact that in p polarization the electric field is continuous at the end of the cylinder; thus the end does not have a large influence on the field computed around the cylinder. However, in s polarization the field is discontinuous at the end of the cylinder and then the field will strongly vary around this end and so will do the force. This is why in s polarization it is necessary to consider cylinders with large lengths in order to avoid edge effects. Now let us address the presence of the plane surface to compute the force. We consider the cylinder length $L=1551$ nm. Like for the sphere, we address both $\theta=0°$ (Fig. 5), and 42° (Fig. 6). The curves from CDM-B stop at $z=10$ nm due to the disadvantage previously noted.

Concerning Fig. 5, if we focus on F_z for p polarization, we can write this force approximated from Eq. (20) by

$$F_z=\frac{4z_0^4|E_0|^2}{|2z_0^2+\alpha_1\Delta|^2}\left((\alpha_1^0)^2k_0^3\pi/4+\frac{(\alpha_1^0)^2\Delta}{4z_0^3}\right). \tag{25}$$

Equation (25) is of the same form as Eq. (22). Hence, the same consequence is derived: near the surface the cylinder is attracted towards the plane surface. But far from the plane the cylinder is pushed away because at this distance the cylinder cannot interact with itself. As with the sphere, we can compute the distance z_0 at which the force is null,

$$z_0^3=\frac{(\varepsilon-1)}{\pi k_0^3(\varepsilon+1)}, \tag{26}$$

which in our illustration leads to $z_0=50$ nm. Although we do not present now an enlargement with details of Fig. 5, we

TABLE III. The same as in Table II but for the electric field parallel to the axis of the cylinder.

CDM-A			CDM-B			Dipole. approx.		Mie
Force	L (nm)	% (Mie)	Force	L (nm)	% (Mie)	Force	% (Mie)	Force
0.5649×10^{-12}	197	63	0.2163×10^{-12}	197	86	1.5015×10^{-12}	2.31	1.5370×10^{-12}
0.9986×10^{-12}	391	35	1.0021×10^{-12}	391	35			
1.3059×10^{-12}	777	15.0	1.3103×10^{-12}	777	14.7			
1.3971×10^{-12}	1164	9.10	1.4018×10^{-12}	1164	8.80			
1.4430×10^{-12}	1551	6.12	1.4479×10^{-12}	1551	5.80			

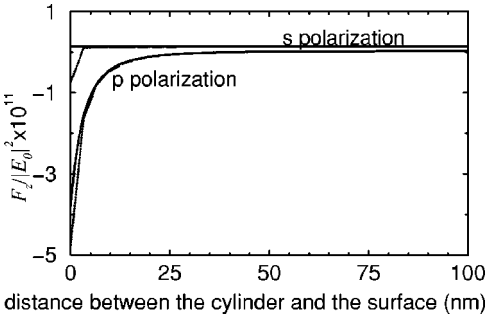

FIG. 5. Normalized force in the Z direction on a cylinder with radius $a=10$ nm, $\lambda=632.8$ nm, and $\varepsilon=2.25$. The light angle of incidence is $\theta=0°$. The full line corresponds to the dipole approximation, the dashed line to the CDM-A, and the dotted line to the CDM-B.

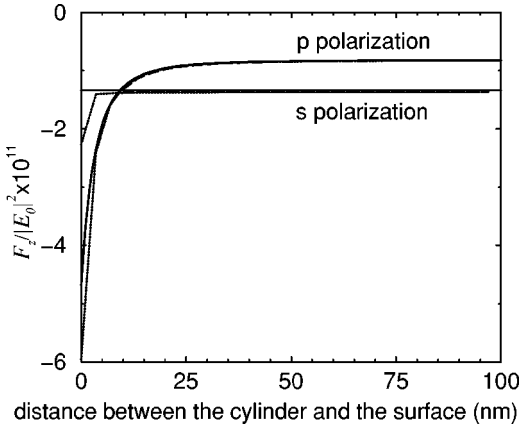

FIG. 6. Normalized force in the Z direction on the same cylinder as described in Fig. 5 but with an angle of incidence $\theta=42°$ larger than the critical angle $\theta_c=41.8°$. The full line corresponds to the dipole approximation, the dashed line to the CDM-A, and the dotted line to the CDM-B.

have found the value $z_0=(40+10)$ nm$=50$ nm. The cylinder in p polarization has the same behavior as the sphere. However, in s polarization there is a difference. Then the force obtained from the dipolar approximation is always constant because there is no interaction with the surface. This is clear from Eq. (19), and it is due to the fact that in the electrostatic limit S_{yy} tends to zero, and then there is no influence of the surface on the cylinder. This is a consequence of the continuity of both the field and its derivative of both the plane and the cylinder.[38] Therefore, the cylinder does not feel the presence of the plane. As the wave is propagating, the force is positive, thus pushing the cylinder away from the plane with magnitude values given by Table III. Notice that the force obtained from CDM-B, when the cylinder is in contact with the surface, becomes negative in s polarization. This is due to the diffraction of the field at the end of the cylinder, which induces a component perpendicular to the plane, and therefore an attractive force.

In the case represented in Fig. 6, as for the sphere, we observe a force always attractive ($F_z<0$) whatever the polarization. For p polarization we have exactly the same behavior as for the sphere. However, for s polarization the normalized force is always constant whatever the distance between the cylinder and the surface, due to the same reason as before, namely, $S_{yy}=0$. Only when the cylinder is on the surface can we see from the CDM-B calculation that the force is slightly more attractive for the same reason previously quoted.

C. Results for a sphere beyond the Rayleigh regime

Let us now consider a sphere of radius $a=100$ nm. This size is far from the Rayleigh scattering regime ($\approx\lambda/3$). As in previous cases, we first validate our method with the aid of Mie's calculation in free space. Table IV shows the results. As before, as d decreases, the CDM results tend to the Mie calculation, the error never exceeding 1.7%. Now, we address the presence of a flat dielectric surface. The forces, to be shown next, are computed with CDM-B only since the particle can be in contact with the surface.

In Fig. 7 we present the case for $\theta=0°$. We have plotted two curves: the exact calculation and the SALRS done with $N=1791$. In the inset of Fig. 7, we see that even near the surface SALRS is not good. This is due to the large radius of the sphere; then the discretization subunits on the top of the sphere are at 100 nm from the surface, and thus the effects of retardation are now important. The SALRS calculation also shows that at a distance of 200 nm (which corresponds to the size of the sphere: $2a=200$ nm) the sphere does not ''feel'' the surface, as manifested by the fact that then the curve obtained from this computation reaches the Mie scattering limit previously obtained in Table IV (cf. the full horizontal line in the inset). Hence, we conclude that evanescent waves are absent from the interaction process at distances beyond this limit. From the exact calculation we obtain a very low force near the surface, due to the interaction of the sphere with itself. This effect vanishes beyond $z\approx 50$ nm where oscillations of the force F_z take place with period $\lambda/2$. As these oscillations do not occur in the SALRS, this means that they are due to interferences from multiple reflections between the surface and the sphere. As expected, they decrease as the sphere goes far from the surface.

TABLE IV. Force on a sphere of radius $a=100$ nm in free space. Numerical results are for different number of subunits N in CDM-A and CDM-B. Comparison with Mie's calculation also given.

CDM-A			CDM-B			Mie
Force	N (d in nm)	% (Mie)	Force	N (d in nm)	% (Mie)	Force
2.1355×10^{-16}	280 (25)	1.31	2.1439×10^{-16}	280 (25)	1.71	2.1080×10^{-16}
2.1353×10^{-16}	912 (17)	1.30	2.1402×10^{-16}	912 (17)	1.53	
2.1332×10^{-16}	1791 (13)	1.20	2.1367×10^{-16}	1791 (13)	1.37	
2.1312×10^{-16}	4164 (10)	1.11	2.1333×10^{-16}	4224 (10)	1.21	

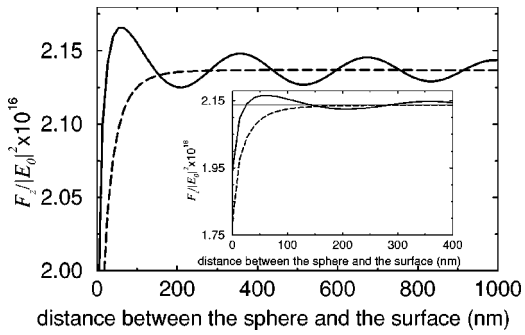

FIG. 7. Normalized force in the Z direction on a sphere with radius $a=100$ nm, $\lambda=632.8$ nm, and $\varepsilon=2.25$. The light angle of incidence is $\theta=0°$. The full line corresponds to the exact calculation with CDM-B, and the dashed line represents the static approximation.

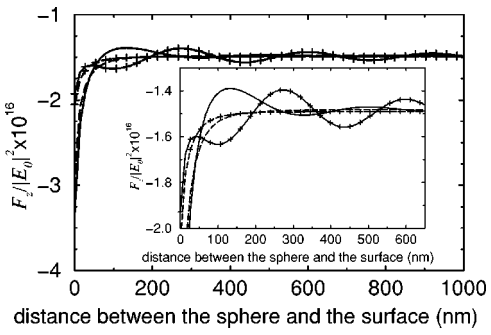

FIG. 8. Normalized force in the Z direction on a sphere with radius $a=100$ nm, $\lambda=632.8$ nm, and $\varepsilon=2.25$. The light angle of incidence is $\theta=42°>\theta_c$. The full line corresponds to the exact calculation with CDM-B, and the dashed line to the static approximation. The curves without symbol are in p polarization, and those with the $+$ symbol in s polarization.

Figure 8 shows the force computed with an angle of incidence $\theta=42°$. We plot the exact calculation (full line) and the SALRS (dashed line) both for p polarization (no symbol) and s polarization ($+$ symbol). Once again, we see that the SALRS is not adequate even near the surface. On the other hand, in the exact calculation, the two polarizations show oscillations of the force F_z with period $\lambda/2$. However, there is a large difference of magnitude of these oscillations between the two polarizations (see inset of Fig. 8). To understand this difference, we must recall that the sphere is a set of dipoles. When a dipole is along the Z direction there is no propagating wave in this direction. But if the dipole is oriented in the X (or Y) direction, its radiation is maximum in the Z direction. However, in s polarization all dipoles are, approximately, parallel to the surface, so there is an important radiation from the dipole in the Z direction and consequently between the sphere and the surface.

V. CONCLUSIONS

In this paper we have presented exact three-dimensional calculations based on the coupled dipole method and an analytical expression for the force on either a sphere or an infinite cylinder, both in front of a flat dielectric surface. The results for electrically small bodies show that, whatever the polarization, in the case of a sphere, and in p polarization for the cylinder, the force always has the same behavior: namely, in the case of illumination under total internal reflection, the particle is always attracted towards the surface. A surprising result in the case when the illuminating beam is perpendicular to the surface and the object remains stuck to the surface is that the force is attractive due the interaction of the particle with itself, and therefore this object keeps stuck to the surface. However, when the object is far from the surface, the force becomes repulsive, as one would have expected.

For s polarization, the cylinder does not ''feel'' the presence of the substrate. This is more noticeable for a propagating wave, namely, at angles of incidence lower than the critical angle. However, when an evanescent wave is created by total internal reflection, the force is attractive under s polarization.

The scope of the static calculation for this configuration has been validated. We have also shown the advantage of having an analytical form that shows the contribution of the incident field on the particle, as well as that of the force induced by the sphere (or cylinder) on itself, thus yielding a better understanding of the physical process involved.

For bigger spheres, we have observed somewhat different effects of the forces. Under the action of evanescent waves, the force is always attractive, but it always becomes repulsive when it is due to propagating waves. Unlike the case of the small sphere, there is no point of zero force.

ACKNOWLEDGMENTS

This work has been supported by the European Union, Grant No. ERBFMRXCT 98-0242 and by the DGICYT, Grant No. PB 98-0464. The authors would like to thank J.-J Greffet and R. Carminati for helpful and valuable discussions. One of us, P. C., is particularly grateful to A. Rahmani for many constructive discussions.

[1] A. Ashkin, Phys. Rev. Lett. **24**, 56 (1970).
[2] A. Ashkin, Phys. Rev. Lett. **25**, 1321 (1970).
[3] A. Ashkin, J.M. Dziedzic, J.E. Bjorkholm, and S. Chu, Opt. Lett. **11**, 288 (1986).
[4] A. Ashkin, J.M. Dziedzic, and T. Yamane, Nature (London) **330**, 769 (1987).
[5] S.M. Block, D.F. Blair, and H.C. Berg, Nature (London) **338**, 514 (1989).
[6] A. Ashkin, Proc. Natl. Acad. Sci. USA **94**, 4853 (1997).
[7] L. Novotny, R.X. Bian, and X. Sunney Xie, Phys. Rev. Lett. **79**, 645 (1997).
[8] M. Tanaka, and K. Tanaka, J. Opt. Soc. Am. A **15**, 101 (1998).
[9] M. Renn, and R. Pastel, J. Vac. Sci. Technol. B **16**, 3859 (1998).
[10] K. Svoboda and S. Block, Opt. Lett. **19**, 930 (1994).
[11] T. Sugiura, T. Okada, Y. Inouye, O. Nakamura, and S. Kawata, Opt. Lett. **22**, 1663 (1997).
[12] R. Omori, T. Kobayashi, and A. Suzuki, Opt. Lett. **22**, 816 (1997).

[13] M. Burns, J.-M. Fournier, and J. Golovchenko, Phys. Rev. Lett. **63**, 1233 (1989).
[14] M. Gu and P. Ke, Appl. Phys. Lett. **75**, 175 (1999).
[15] M.I. Antonoyiannakis and J.B. Pendry, Phys. Rev. B **60**, 2363 (1999).
[16] M.I. Antonoyiannakis, and J.B. Pendry, Europhys. Lett. **40**, 613 (1997).
[17] M. Bayer, T. Gutbrod, A. Forchel, T.L. Reinecke, P.A. Knipp, A.A. Dremin, V.D. Kulakovskii, and J.P. Reithmaier, Phys. Rev. Lett. **81**, 2582 (1997).
[18] S. Kawata and T. Sugiura, Opt. Lett. **17**, 772 (1992).
[19] E. Almaas and I. Brevik, J. Opt. Soc. Am. B **12**, 2429 (1995).
[20] M. Lester and M. Nieto-Vesperinas, Opt. Lett. **24**, 936 (1999).
[21] K. Visscher and G.J. Brakenhoff, Optik (Stuttgart) **89**, 174 (1992).
[22] J.P. Barton, D.R. Alexander, and S.A. Scaub, J. Appl. Phys. **66**, 4594 (1989).
[23] S. Chang, J.H. Jo, and S.S. Lee, Opt. Commun. **108**, 133 (1994).
[24] C.E. Dungey and C.F. Bohren, J. Opt. Soc. Am. A **8**, 81 (1991).
[25] P.C. Chaumet, A. Rahmani, F. de Fornel, and J.-P. Dufour, Phys. Rev. B **58**, 2310 (1998).
[26] E.M. Purcell and C.R. Pennypacker, Astrophys. J. **186**, 705 (1973).
[27] J.D. Jackson, *Classical Electrodynamics*, 2nd ed. (Wiley, New York, 1975), p. 395.
[28] A. Rahmani (private communication).
[29] G.S. Agarwal, Phys. Rev. A **11**, 230 (1975); **12**, 1475 (1975).
[30] A. Rahmani, P.C. Chaumet, F. de Fornel, and C. Girard, Phys. Rev. A **56**, 3245 (1997).
[31] B.T. Draine, Astrophys. J. **333**, 848 (1988).
[32] P.C. Chaumet and M. Nieto-Vesperinas (unpublished).
[33] In fact **F** is the time averaged force on the particle.
[34] J.A. Stratton, *Electromagnetic Theory* (McGraw-Hill, New York, 1941).
[35] J.P. Gordon, Phys. Rev. A **8**, 14 (1973).
[36] A. Lakhtakia, Int. J. Mod. Phys. C **34**, 583 (1992).
[37] A.D. Yaghjian, Proc. IEEE **68**, 248 (1980).
[38] F. Pincemin, A. Sentannac, and J.-J. Greffet, J. Opt. Soc. Am. A **11**, 1117 (1994).
[39] J.-J. Greffet, Opt. Commun. **72**, 274 (1989).
[40] H.C. van de Hulst, *Light Scattering by Small Particles* (Dover, New York, 1981).